The Reductase of *p*-Hydroxyphenylacetate 3-Hydroxylase from *Acinetobacter baumannii* Requires *p*-Hydroxyphenylacetate for Effective Catalysis†

Jeerus Sucharitakul,‡ Pimchai Chaiyen,*,‡ Barrie Entsch,§ and David P. Ballou§

Department of Biochemistry and Center for Excellence in Protein Structure and Function, Faculty of Science, Mahidol University, Rama 6 Road, Bangkok, Thailand, and Department of Biological Chemistry, University of Michigan, Ann Arbor, Michigan 48109

Received April 4, 2005; Revised Manuscript Received June 13, 2005

ABSTRACT: *p*-Hydroxyphenylacetate (HPA) hydroxylase (HPAH) from *Acinetobacter baumannii* catalyzes hydroxylation of HPA to form 3,4-dihydroxyphenylacetate. It is a two-protein system consisting of a smaller reductase component (C_1) and a larger oxygenase component (C_2). C_1 is a flavoprotein containing FMN, and its function is to provide reduced flavin for C_2 to hydroxylate HPA. We have shown here that HPA plays important roles in the reaction of C_1. The apoenzyme of C_1 binds to oxidized FMN tightly with a K_d of 0.006 μM at 4 °C, but with a K_d of 0.038 μM in the presence of HPA. Reduction of C_1 by NADH occurs in two phases with rate constants of 11.6 and 3.1 s^{-1} and K_d values for NADH binding of 2.1 and 1.5 mM, respectively. This result indicates that C_1 exists as a mixture of isoforms. However, in the presence of HPA, the reduction of C_1 by NADH occurred in a single phase at 300 s^{-1} with a K_d of 25 μM for NADH binding at 4 °C. Formation of the C_1−HPA complex prior to binding of NADH was required for this stimulation. The redox potentials indicate that the rate enhancement is not due to thermodynamics ($E°_m$ of the C_1−HPA complex is −245 mV compared to an $E°_m$ of C_1 of −236 mV). When the C_1−HPA complex was reduced by 4(*S*)-NADH, the reduction rate was changed from 300 to 30 s^{-1}, giving a primary isotope effect of 10 and indicating that C_1 is specifically reduced by the *pro*-(*S*)-hydride. In the reaction of reduced C_1 with oxygen, the reoxidation reaction is also biphasic, consistent with reduced C_1 being a mixture of fast and slow reacting species. Rate constants for both phases were the same in the absence and presence of HPA, but in the presence of HPA, the equilibrium shifted toward the faster reacting species.

p-Hydroxyphenylacetate hydroxylase (HPAH)[1] catalyzes hydroxylation of *p*-hydroxyphenylacetate (HPA) to form 3,4-dihydroxyphenylacetate (DHPA). This hydroxylation is usually found as the initial step in the aerobic degradation pathway for HPA, one of the major metabolites of lignin (*1*). In the past decade, it has been revealed that the hydroxylation of HPA in various organisms is carried out by at least three different types of two-protein component enzyme systems (*2*−*4*). The first HPAH purified was from *Pseudomonas putida* and shown to be a two-protein component enzyme system (*2*). Studies of *P. putida* HPAH have shown that FAD is tightly bound to the smaller component and that the larger component appears to be a coupling protein enabling hydroxylation (*2*, *5*). The reaction with NADH and that with oxygen and substrate were reported to occur on the flavoprotein component. The mechanism of *P. putida* HPAH seems to be similar to the mechanism of single-component aromatic flavoprotein hydroxylases except that two proteins are required (*5*−*7*). A different HPAH system was later isolated from *Escherichia coli* W, and studies have shown that the smaller component of *E. coli* HPAH (HpaC) is a flavin reductase generating free reduced FAD that is transferred to the larger component (HpaB) to hydroxylate HPA (*3*, *8*). It was shown that several different flavin reductases could replace HpaC in the reaction of *E. coli* HPAH (*8*, *9*).

We have isolated HPAH from *Acinetobacter baumannii* and showed that the enzyme is quite different from the analogous HPAH enzymes from both *P. putida* and *E. coli* (*4*, *10*). The *A. baumannii* HPAH is a two-protein enzyme system consisting of a smaller reductase component (C_1) and a larger oxygenase component (C_2) (*4*). The enzyme was

† Financial support was received from The Thailand Research Fund Grants RSA/09/2545 and RTA4780006 and Mahidol University (to P.C.) and NIH Grant GM64711 (to D.P.B.). J.S. is a recipient of a scholarship under the Commission on Higher Education Staff Development Project, Mahidol University. This study was also partly supported by a Research Team Strengthening Grant from BIOTECH to Skorn Mongkolsuk.

* To whom correspondence should be addressed. E-mail: scpcy@mucc.mahidol.ac.th. Phone: 66-2201-5607. Fax: 66-2354-7174.

‡ Mahidol University.

§ University of Michigan.

[1] Abbreviations: HPA, *p*-hydroxyphenylacetate; HPAH, *p*-hydroxyphenylacetate hydroxylase; C_1, reductase component of HPAH from *A. baumannii*; C_2, oxygenase component of HPAH from *A. baumannii*; HpaC, reductase component of HPAH from *E. coli*; HpaB, oxygenase component of HPAH from *E. coli*; NTA, nitrilotriacetate; cB, reductase component of NTA monooxygenase from *Aminobacter aminovorans*; PheA, phenol hydroxylase from *Bacillus thermoglucosidasius* A7; PheA2, reductase component of PheA; C_1^{red}, reduced form of C_1; C_1−HPA, complex of C_1 and HPA; C_1^{red}−HPA, complex of C_1^{red} and HPA; C_1−HPA:NADH, charge-transfer complex of C_1−HPA and NADH; C_1^{red}−HPA:NAD^+, charge-transfer complex of C_1^{red}−HPA and NAD^+; 4(*R*)-NADD, deuterated 4(*R*)-[^{2}H]NADH; 4(*S*)-NADD, deuterated 4(*S*)-[^{2}H]NADH; apoC_1, apoenzyme of C_1; k_{obs}, apparent rate constant; FMN, flavin mononucleotide; $FMNH^-$, reduced flavin mononucleotide.

10.1021/bi050615e CCC: $30.25
Published on Web 07/12/2005

recently cloned and expressed in *E. coli* (*10*). Sequence and biochemical analyses indicate that the enzyme represents a novel prototype of enzymes in the two-protein component class of aromatic hydroxylases. C_1 is a flavoprotein enzyme having FMN bound tightly (*4*), in contrast to HpaC from *E. coli* that is reported not to bind tightly to any flavins (*3*). Moreover, HPA, a substrate of the C_2 component, was found to increase the rate of NADH oxidation by C_1 (*4*). By contrast, HPA does not have any effect on the HpaC reaction (enzyme system from *E. coli*) (*3*).

Several flavoprotein hydroxylases that have separate reductase/oxygenase components such as those of *A. baumannii* and *E. coli* HPAH have been characterized recently, including phenol hydroxylase (PheA) from both *Bacillus stearothermophilus* BR219 and *Bacillus thermoglucosidasius* A7 (*11*, *12*), chlorophenol 4-monooxygenase from *Burkholderia cepacia* AC1100 (*13*), 2,4,6-trichlorophenol monooxygenase from *Ralstonia eutropha* JMP134 (*14*), pyrrole-2-carboxylate monooxygenase from *Rhodococcus* sp. (*15*), styrene monooxygenase from *Pseudomonas* VLB120 (*16*), and *p*-nitrophenol hydroxylase from *Bacillus sphaericus* (*17*). In addition to the hydroxylation of aromatic substrates, two-component flavoprotein hydroxylases are found to oxygenate aliphatic compounds; these include nitrilotriacetate (NTA) monooxygenase (*18*, *19*), EDTA monooxygenase (*20*), alkane sulfonate monooxygenase (*21*), and bacterial luciferase (aldehyde monooxygenase) (*22*, *23*). Flavoprotein oxygenases with two protein components are also involved in the biosynthesis of the antibiotics actinorhodin (*24*, *25*), pristinamycin IIA (*26*), and valanimycin (*27*). Genome sequencing projects have identified many putative proteins as homologues of these two-component enzymes, indicating their vital roles in a wide variety of microorganisms.

Reaction mechanisms of two-component enzymes are not well understood. In this study, we have investigated the thermodynamics and kinetics of reactions of C_1 in the presence and absence of HPA. Results are presented for the binding of FMN to apoC_1 and the binding of HPA to C_1 and for the redox potentials of C_1 and the C_1−HPA complex. Kinetic data demonstrate the role of HPA in controlling the reactivity of C_1, both in its reduction by NADH and in its oxidation by oxygen. Subsequent papers will describe the properties of C_2 and the combined function of C_1 and C_2 in achieving hydroxylation of HPA in the cellular environment.

MATERIALS AND METHODS

Reagents. NAD^+, NADH, glucose, glucose oxidase, and superoxide dismutase were from Sigma. Pure FMN was obtained by hydrolyzing FAD with phosphodiesterase from the venom of the snake *Crotalus adamanteus* (*28*). In brief, FAD (2.5 mg/mL) and venom (50 μg/mL) in 20 mM potassium phosphate buffer (pH 7.0) were incubated overnight in the dark. The reaction mixture was loaded onto a C18 Sep-Pak cartridge (Waters), previously equilibrated with 20 mM potassium phosphate buffer (pH 7.0), and the cartridge was washed with 10 mM potassium phosphate buffer (pH 7.0). FMN was eluted with water, and the solution was freeze-dried. Deuterated formic acid (^{2}HCOOH, 98%) and deuterated D-glucose [$HOCH_2(CHOH)_4C^2HO$, 98%] were obtained from Cambridge Isotope Laboratories. 4(*S*)-NADD was synthesized by using deuterated glucose, hexokinase (1 mg/mL), glucose-6-phosphate dehydrogenase, and 100 mM ATP. Deuterated glucose was converted to deuterated glucose 6-phosphate by hexokinase, and NAD^+ was converted to 4(*S*)-NADD by using deuterated glucose 6-phosphate and glucose-6-phosphate dehydrogenase. Likewise, 4(*R*)-NADD was synthesized by using formate dehydrogenase to catalyze the reduction of NAD^+ to 4(*R*)-NADD by deuterated formate (*29*). Each product was purified from the reaction mixture using AG-MP1 anion-exchange resin (100−200 mesh, chloride form) from Bio-Rad (*30*). The concentrations of the following compounds were determined using known extinction coefficients at pH 7.0: $\epsilon_{340} = 6.22 \times 10^3$ M^{-1} cm^{-1} for NADH and NADD, $\epsilon_{446} = 12.2 \times 10^3$ M^{-1} cm^{-1} for FMN, and $\epsilon_{277} = 1.55 \times 10^3$ M^{-1} cm^{-1} for HPA (*4*). C_1 used in this study was cloned, expressed, and prepared as previously described (*4*, *10*). The concentration of the purified enzyme was measured using an ϵ_{458} of 12.8 $\times 10^3$ M^{-1} cm^{-1} (per enzyme-bound FMN).

Spectroscopic Studies. UV−visible absorbance spectra were recorded with a Hewlett-Packard diode array spectrophotometer (HP 8453A), or a Shimadzu 2501PC spectrophotometer. Fluorescence measurements were carried out with a Shimadzu RF5301PC spectrofluorometer. All spectral instruments were equipped with thermostated cell compartments.

Rapid Reaction Experiments. Reactions were carried out in 50 mM sodium phosphate buffer (pH 7.0) at, 4 °C, unless otherwise specified. Rapid kinetics measurements were performed with Hi-Tech Scientific model SF-61DX or model SF-61SX stopped-flow spectrophotometers in single mixing mode. The optical path lengths of the observation cells were 1 cm. The stopped-flow apparatus was made anaerobic by flushing the flow system with an anaerobic buffer solution containing glucose and glucose oxidase. This solution was composed of 400 μM glucose, 1 μg/mL glucose oxidase, and 4.8 μg/mL catalase in 50 mM sodium phosphate buffer (pH 7.0). The buffer was made anaerobic by equilibrating with oxygen-free argon or nitrogen that had been passed through an Oxyclear oxygen removal column (Labclear). The anaerobic buffer was allowed to stand in the flow system overnight. The flow unit was then rinsed with anaerobic buffer before the experiments. Apparent rate constants (k_{obs}) from kinetic traces were calculated from exponential fits using KinetAsyst3 (Hi-Tech Scientific, Salisbury, U.K.) or program A (written at the University of Michigan by Rong Chang, Jung-yen Chiu, Joel Dinverno, and D. P. Ballou). For studying the reduction of C_1 by NADH or NADD, enzyme or enzyme−HPA complexes were placed in tonometers and equilibrated with argon or nitrogen (*31*)**.** The enzyme solution also contained 200 μM glucose, 1 μg/mL glucose oxidase, and 4.8 μg/mL catalase to eliminate traces of oxygen. NADH or NADD solutions were placed in glass syringes and made anaerobic by bubbling with oxygen-free argon for ≥6 min before being loaded onto the stopped-flow machine. For studying the reaction of reduced C_1 with oxygen, the anaerobic enzyme solution in a glass tonometer was reduced with a solution of sodium dithionite [~5 mg/mL in 100 mM potassium phosphate buffer (pH 7.0)] delivered from a syringe attached to the tonometer. Reduction was monitored by following the flavin absorbance. Solutions with various concentrations of oxygen were prepared by equilibrating buffer with air or with certified oxygen-in-

nitrogen gas mixtures. Determinations of rate constants were obtained from the plots of k_{obs} versus substrate concentration using a Marquardt−Levenberg nonlinear fit algorithm that is included in KaleidaGraph (Synergy Software).

Redox Potential Determinations. Redox potentials of C_1-bound FMN, in the presence or absence of HPA in 50 mM sodium phosphate buffer (pH 7.0) at 25 °C, were determined by the method of Massey (*32*). Xanthine and xanthine oxidase were used to catalytically reduce the enzyme with benzyl viologen as an electron mediator. The dye employed as a reference potential for the determination of redox potentials for both C_1 and C_1−HPA complexes was phenosafranine [$E°_m = -252$ mV (*33*)]. During the reduction process, absorbance at wavelengths of 458 and 521 nm was used to calculate the amount of oxidized enzyme and dye. Because dye and enzyme absorb at both wavelengths, eqs 1 and 2 were used to calculate the concentration of each species.

$$A_{458} = \epsilon^{E}_{458} c^{E} + \epsilon^{D}_{458} c^{D} \quad (1)$$

$$A_{521} = \epsilon^{E}_{521} c^{E} + \epsilon^{D}_{521} c^{D} \quad (2)$$

The values of molar absorption coefficients are as follows: ϵ^{E}_{458} (oxidized enzyme at 458 nm) $= 12.8 \times 10^3$ M^{-1} cm^{-1}, ϵ^{E}_{521} (oxidized enzyme at 521 nm) $= 0.48 \times 10^3$ M^{-1} cm^{-1}, ϵ^{D}_{458} (oxidized dye at 458 nm) $= 10.8 \times 10^3$ M^{-1} cm^{-1}, and ϵ^{D}_{521} (oxidized dye at 521 nm) $= 44.7 \times 10^3$ M^{-1} cm^{-1}.

Preparation of the Apoenzyme of C_1 (ApoC_1). Approximately 6.8 mg of C_1 was applied onto a phenyl-Sepharose column (1.3 cm × 3 cm) equilibrated with 15% ammonium sulfate in 50 mM sodium phosphate buffer (pH 7.0), 1 mM DTT, and 0.5 mM EDTA at 4 °C. The column was then washed with 400 mL of 15% ammonium sulfate in 50 mM sodium phosphate buffer (pH 3.5), 1 mM DTT, and 0.5 mM EDTA to elute free FMN from the holoenzyme. The apoenzyme was eluted with 40% ethylene glycol in 10 mM sodium phosphate, 1 mM DTT, and 0.5 mM EDTA (pH 9.0). ApoC_1 was concentrated, and gel filtration was used to exchange into the buffer appropriate for stopped-flow experiments. The apoenzyme concentration was measured using the extinction coefficient at 280 nm ($\epsilon_{280} = 27.2 \times 10^3$ M^{-1} cm^{-1}).

Determination of the Dissociation Constant (K_d) of the C_1−FMN Complex in the Absence and Presence of HPA. Binding experiments were performed by an ultrafiltration method using a Centriprep unit with a molecular mass cutoff of 30 kDa (Amicon). A solution of 8 μM C_1 (total volume of 15 mL) in 50 mM sodium phosphate buffer (pH 7.0) was placed in the Centriprep unit, and centrifuged at 3200 rpm for 15 min at 4 °C. Approximately 1 mL of filtrate was separated into the filtrate chamber after this centrifugation condition, and was used for measuring the free FMN concentration by fluorescence, with excitation at 446 nm and emission at 525 nm. The K_d value was calculated from the ratio of free species to the complex. Similar experiments were performed in the presence of various concentrations of HPA: 10, 20, 40, and 100 μM. K_d values of the C_1−FMN complex at each concentration of HPA were defined as K_d^{app}.

RESULTS

Binding of FMN to ApoC_1. The kinetics of binding of FMN to apoC_1 were measured by monitoring the fluorescence change of FMN upon mixing the two compounds in the stopped-flow apparatus. Results showed that the fluorescence of the FMN was quenched upon binding to the enzyme, and the change appeared to be monophasic (Figure 1). The observed rate constants for the binding reactions were linearly dependent on the concentrations of apoC_1 (inset of Figure 1), indicating that the binding is a one-step reaction with a k_{on} (slope of the plot) of 9.0×10^5 M^{-1} s^{-1} and a k_{off} value (intercept of the plot) close to zero. The dissociation constant (K_d) for the C_1−FMN complex was measured using an ultrafiltration method to measure the amount of free FMN dissociating from the complex. From the results, a K_d of 0.006 μM was obtained, giving a calculated value of 0.0054 s^{-1} for k_{off}.

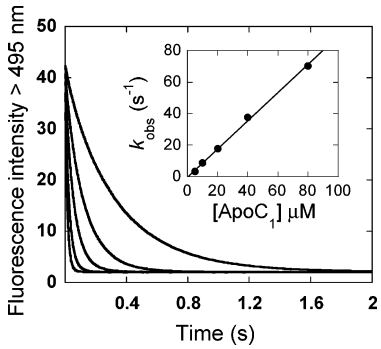

FIGURE 1: Kinetics of binding of apoC_1 to FMN. FMN (0.5 μM final) was mixed with apoC_1 at concentrations after mixing of 5, 10, 20, 40, and 80 μM (traces from right to left) in 50 mM sodium phosphate buffer (pH 7.0) at 4 °C. The fluorescence of FMN was monitored with excitation at 446 nm and detecting emission at >495 nm. The inset shows that the observed rate constants from kinetic traces are linearly dependent on apoC_1 concentration, indicating a one-step binding process with a k_{on} (slope) of 9.0×10^5 M^{-1} s^{-1} and a k_{off} (intercept) close to zero.

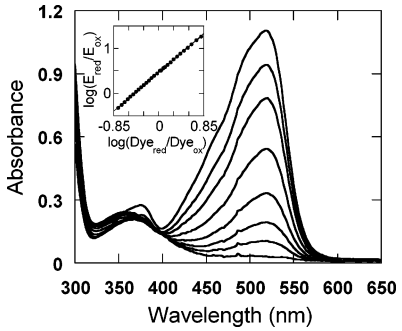

FIGURE 2: Redox potential measurements of C_1. Enzyme (23 μM) and phenosafranine (23 μM) in 50 mM sodium phosphate buffer (pH 7.0) at 25 °C were slowly reduced by the xanthine/xanthine oxidase system (400 μM xanthine, 0.01 unit of xanthine oxidase, and 5 μM benzyl viologen). The reaction was followed spectrally for 6 h, and absorbance values at 458 and 521 nm were used to calculate the amount of oxidized dye and enzyme at different times (Materials and Methods). The inset shows that the plot of log(E_{red}/E_{ox}) vs log(dye$_{red}$/dye$_{ox}$) yielded a slope of 1 (overlaid line is a linear fit with a slope of 1). The redox potential value was calculated to be −236 mV.

Determination of Redox Potential Values for C_1 and the C_1−HPA Complex. The redox potential of FMN bound to C_1 and the C_1−HPA complex was determined by the method of Massey (*32*) using phenosafranine as the reference dye ($E°_m = -252$ mV) as described in Materials and Methods and shown in Figure 2. The spectra obtained in the analysis indicated that both the enzyme and dye were reduced by

xanthine and xanthine oxidase via a two-electron reduction process. It is possible that any semiquinones formed were rapidly disproportionated by the electron mediator, benzyl viologen, included in the reaction. Absorbance at wavelengths of 458 and 521 nm was used to calculate the amount of oxidized dye and enzyme as described in Materials and Methods. The midpoint potentials ($E°_m$) calculated from the plots of log(E_{red}/E_{ox}) and log(dye_{red}/dye_{ox}) are −236 mV for C_1 (inset of Figure 2) and −245 mV for the C_1−HPA complex (determined in the presence of 400 μM HPA, data not shown). The slopes of both plots have values close to unity, again indicating that the traces during reduction represented points of true equilibrium between the dye and enzyme. Measurements of redox potential were also carried out using anthraquinone 1-sulfonate ($E°_m = -218$ mV) as another reference dye under the same conditions for reductions. The results indicate that anthraquinone 1-sulfonate is reduced faster than the enzyme and confirm that the redox potential of C_1 is −236 mV. The redox potentials, which are both lower than that of free FMN at pH 7.0 (−219 mV) (*33*), show that $FMNH^-$ is bound less tightly to C_1 than is FMN, and the presence of HPA accentuates this difference. Thus, both reduction of the flavin and binding of HPA promote release of $FMNH^-$ from C_1, a possible mechanism for delivering $FMNH^-$ to C_2.

Binding of HPA to C_1. Although HPA is not a substrate for C_1, it serves as an effecter of catalysis by enhancing the rate of flavin reduction by NADH (*4*). Adding HPA to the enzyme resulted in an increase in flavin fluorescence and a decrease in the intensity of the 450 nm absorption band. The kinetics of binding of HPA to C_1 were investigated by mixing C_1 with HPA in the stopped-flow spectrofluorometer and monitoring the change in flavin fluorescence. An increase in flavin fluorescence was observed upon mixing HPA with the protein (data not shown). This change could be due to the intrinsic fluorescence of the C_1−HPA complex being higher than that of C_1, or to weaker binding of FMN to C_1 when HPA was present, so that flavin dissociates from the enzyme. The latter possibility was tested by measuring the amount of free FMN dissociating from the complex in the presence and absence of HPA by using an ultrafiltration method. The K_d for binding of apoC_1 to FMN (free enzyme) is 0.006 ± 0.001 μM. However, more free FMN was detected in the presence of HPA, and this could account for the overall increase in fluorescence, since free FMN is ∼10-fold more fluorescent than C_1-bound FMN. A plot of the apparent dissociation constant (K_d^{app}) values of the C_1−FMN complex versus HPA concentration was hyperbolic (Figure 3), and the K_d^{HPA} for binding of HPA to C_1 was calculated to be 0.9 ± 0.2 μM. From this plot, the maximum value of K_d^{app} (0.038 ± 0.007 μM) represents the K_d for binding of apoC_1 to FMN in the presence of HPA.

Reduction of C_1 by NADH. C_1 was mixed with various concentrations of NADH anaerobically in the stopped-flow spectrophotometer, and the reactions were monitored by absorbance changes at 458 nm, a wavelength that provides the maximum difference between FMN and $FMNH^-$ (Figure 4). The reduction of C_1-bound FMN by NADH resulted in a biphasic decrease in absorbance at 458 nm. The faster phase accounted for ∼50% of the total absorbance change at the lowest NADH concentration (100 μM NADH), and this proportion increased with an increase in NADH concentration. For the highest NADH concentration (10.4 mM NADH), the faster phase accounted for ∼78% of the total absorbance change. Although it is difficult to obtain accurate analysis of the traces composed of two exponential terms with similar amplitude changes, both phases in C_1 reduction were separated by a k_{obs1}/k_{obs2} ratio of ∼4 over all the NADH concentrations that were used. The separation of both phases is slightly above the limit value (the ratio of k_{obs1}/k_{obs2} of 3), allowing reasonable analysis to be carried out by this method (*34*). Apparent rate constants (k_{obs}) for both phases increased at higher concentrations of NADH, and approached limiting values of 11.6 ± 0.3 and 3.06 ± 0.08 s^{-1}, respectively (inset of Figure 4).

One possible explanation for these biphasic kinetics is that C_1 exists in two distinct populations that interconvert slowly, and each reacts with NADH with distinct kinetics and affinity (Scheme 1). Because the rates of reduction in both phases

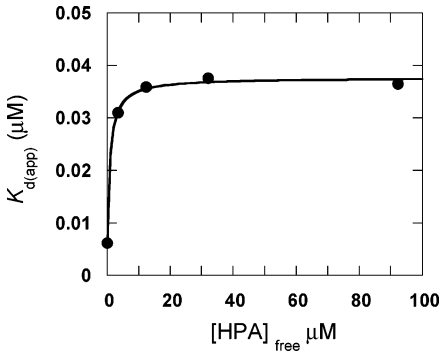

FIGURE 3: Plot of the apparent K_d of the C_1−FMN complex at various concentrations of free HPA. Enzyme (8 μM, final concentration) was incubated with various concentrations of HPA (10, 20, 40, and 100 μM) in 50 mM sodium phosphate buffer (pH 7.0). Each of the reaction mixtures at the indicated HPA concentrations was passed through an ultrafiltration device at 4 °C. The amount of free FMN in the filtrate was determined from its fluorescence intensity at 525 nm. The apparent K_d (K_d^{app}) based on free FMN was hyperbolically dependent on the concentration of HPA included. The concentration of free HPA giving a half-maximal value of the plot represents K_d^{HPA} for binding of HPA to C_1 (0.9 ± 0.2 μM). The maximum value of the plot (0.038 ± 0.007 μM) represents the K_d for binding of apoC_1 to FMN in the presence of HPA.

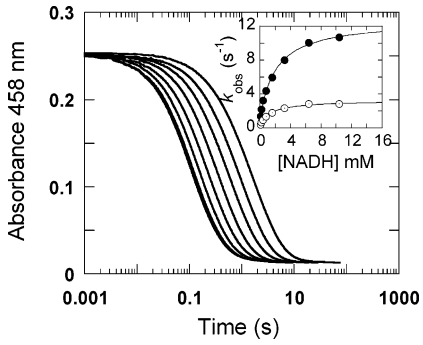

FIGURE 4: Kinetic traces for the reduction of C_1. Reduction of C_1 (20 μM, final concentration) by NADH (0.1, 0.2, 0.4, 0.8, 1.6, 3.2, 6.4, and 10.4 mM after mixing) in 50 mM sodium phosphate buffer (pH 7.0), 1 mM DTT, and 0.5 mM EDTA at 4 °C was monitored in the stopped-flow spectrophotometer at 458 nm. Traces from right to left are from lower to higher concentrations of NADH. Data were fitted with two exponentials. The inset shows that both rate constants (k_{obs}) are hyperbolically dependent on NADH concentration. Calculated rate constants and dissociation constants are reported in Table 1.

Table 1: Kinetic and Thermodynamic Constants of the C_1 Reaction

reaction	rate constant	dissociation constant (K_d)
apoC_1 + FMN	$k_{on} = 9.0 \times 10^5\ M^{-1}\ s^{-1}$ $k_{off} = 0.0054\ s^{-1}$ [a]	$K_d = 0.006 \pm 0.001\ \mu M$
apoC_1 + FMN (in the presence of HPA)	−	$K_d = 0.038 \pm 0.007\ \mu M$
C_1 + HPA	−	$K_d^{HPA} = 0.9 \pm 0.2\ \mu M$
C_1 + NADH	$k_3 = 11.6 \pm 0.3\ s^{-1}$ $k'_3 = 3.06 \pm 0.08\ s^{-1}$	$K_d^{NADH} = 2.1 \pm 0.2$ mM $K'_d{}^{NADH} = 1.5 \pm 0.2$ mM
C_1−HPA + NADH(D)	$k_{1(HPA)} = 4 \times 10^7\ M^{-1}\ s^{-1}$ [b] $k_{2(HPA)} = 1000\ s^{-1}$ [b] $k^H_{3(HPA)} = 300\ s^{-1}$ [c] $k^D_{3(HPA)} = 30\ s^{-1}$ [c] $k_{4(HPA)} = 100\ s^{-1}$	$K_d^{NADH} = 25\ \mu M$
C_1^{red} + O_2 (with or without HPA)	$k_{ox}^{fast} = 820\ M^{-1}\ s^{-1}$ $k_{ox}^{slow} = 320\ M^{-1}\ s^{-1}$	− −

[a] k_{off} was estimated from the dissociation constant (K_d). [b] Rate constants were obtained from simulation. [c] k^H and k^D are the rate constants for NADH and NADD, respectively.

Scheme 1

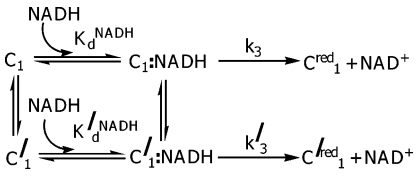

reach limiting values at high concentrations of NADH (inset of Figure 4), it is likely that each type of C_1 reacts with NADH in a two-step process where an initially formed binary complex is followed by reduction in the second step (Scheme 1) (*35*). Data for each phase were analyzed according to eq 3 (*35*)

$$k_{obs} = \frac{k_3[\mathrm{NADH}]}{K_d^{NADH} + [\mathrm{NADH}]} \quad (3)$$

The model in Scheme 1 suggests that one form of C_1 reacts faster with NADH with an intrinsic rate constant for hydride transfer (k_{red} or k_3) of 11.6 ± 0.3 s^{-1} and a dissociation constant (K_d^{NADH}) for NADH of 2.1 ± 0.2 mM, while the other form reacted slower with NADH with a k'_{red} (k'_3) of 3.06 ± 0.08 s^{-1} and a $K'_d{}^{NADH}$ of 1.5 ± 0.2 mM (Table 1).

Reduction of C_1 by NADH in the Presence of HPA. The kinetics of reduction of C_1 by NADH in the presence of HPA were measured by the same methods as described for the absence of HPA (previous section). The C_1−HPA complex was mixed with various concentrations of NADH and monitored in the stopped-flow spectrophotometer at wavelengths of 458 and 690 nm (Figure 5A,B). The reduction was markedly stimulated by HPA; the complete reduction of flavin was achieved within 0.04 s with 80 μM NADH (Figure 5A), whereas 1 s was required for complete reduction of C_1 alone at 10.4 mM NADH (Figure 4). Note that at 80 μM NADH, the reduction took ~20 s without HPA. The first phase of the reaction occurred within the dead time of the stopped-flow machine, as shown by the absorbance present at 690 nm 1 ms after mixing (Figure 5B). The second phase (from ~1 to 10 ms) was the hydride-transfer phase, as indicated by a major loss of absorbance at 458 nm and a small increase at 690 nm. The increase at 690 nm is caused by formation of an $FADH^-$ to NAD^+ charge-transfer complex. The third phase was due to the decay of the charge-transfer species detected at both 458 and 690 nm. Fitting of the data in Figure 5 therefore required three phases with the fastest phase occurring within the dead time of the stopped-flow instrument. The model in Scheme 2 was shown by simulation to fit the data. According to this model, NADH binds to the C_1−HPA complex to form the first charge-transfer species (C_1−HPA:NADH) within the dead time of the instrument. The C_1-bound FMN was subsequently reduced by NADH to form a second charge-transfer species (C_1^{red}−HPA:NAD^+), and the NAD^+ in this complex finally

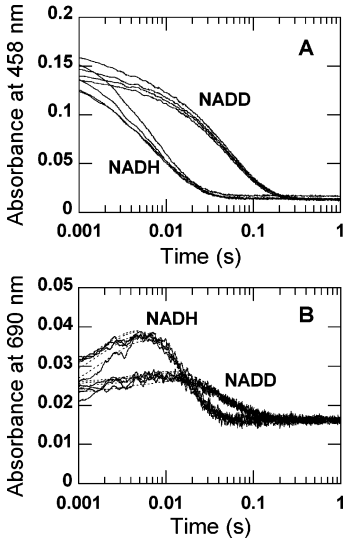

FIGURE 5: Kinetic traces of the reduction of the C_1−HPA complex with NADH. Enzyme (16 μM) and 400 μM HPA were mixed with NADH or 4(*S*)-NADD at concentrations of 80, 160, 320, and 640 μM. All concentrations were after mixing. Reaction conditions were the same as those in Figure 4. The reactions with NADH were those finishing in 0.04 s, and those of 4(*S*)-NADD were complete at 0.3 s. (A) The reaction was monitored at 458 nm. (B) The reaction was monitored at 690 nm. Dotted lines are simulated traces using kinetic constants described in Table 1 and Scheme 2.

Scheme 2

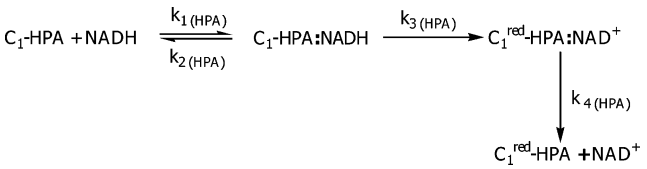

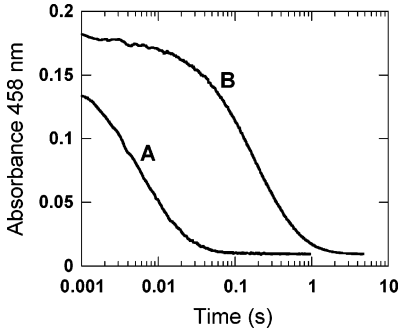

FIGURE 6: Requirement of HPA binding prior to NADH reduction. Trace A was obtained by mixing a solution of C_1 (16 μM) and 200 μM HPA with 10 mM NADH, while trace B was obtained by mixing C_1 (16 μM) alone with the solution of 15 mM NADH and 200 μM HPA. All concentrations were after mixing. The reactions were monitored by stopped-flow spectrophotometry at 458 nm and were carried out in 50 mM sodium phosphate buffer (pH 7.0), 1 mM DTT, and 0.5 mM EDTA at 4 °C.

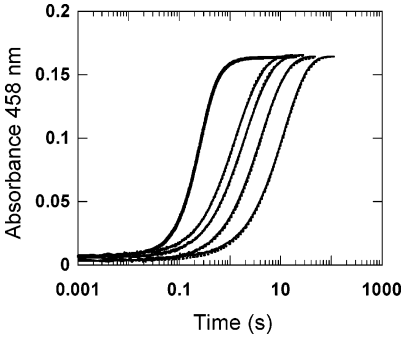

FIGURE 7: Reaction of C_1^{red} with oxygen in the presence of HPA. Reduced C_1 (16 μM, final concentration) with 200 μM HPA (final concentration) was mixed with buffer containing various final oxygen concentrations of 130, 325, 650, and 960 μM in 50 mM sodium phosphate buffer (pH 7.0) at 4 °C. All reaction mixtures contained catalase (0.3 unit) and superoxide dismutase (0.2 unit). The reactions were monitored at selected wavelengths by stopped-flow spectrophotometry. Kinetics were identical at all wavelengths. From right to left, traces represent increasing oxygen concentrations. Dotted lines overlaid are fitted traces using rate constants as indicated in the text. The bold line on the left represents oxidation of 13 μM reduced FMN with 960 μM oxygen.

dissociated with a rate constant of ~100 s^{-1}. This last phase is indicated by the loss of absorbance at 690 nm. The kinetic constants used for simulation of traces in Figure 5 are summarized in Table 1. It should be noted that the reduction of the C_1−HPA complex, unlike the reduction of C_1 alone, can be explained by using a single species of the enzyme as described in Scheme 2. Therefore, the role of HPA in the reduction reaction is to enhance the binding and the rate of reduction by NADH, as well as to stabilize the protein conformation of C_1 required to promote the reduction of the flavin. Similar effects of HPA were found in the reaction of the flavoprotein component of *p*-hydroxyphenylacetate hydroxylase from *P. putida* (*5*). It was observed that in the presence of HPA, the rate of FAD reduction by NADH in the *P. putida* enzyme was increased ~100-fold, and the reduction kinetics were also changed from biphasic to monophasic (*5*).

We have also investigated whether the formation of the C_1−HPA complex was indeed required prior to binding of NADH to attain the full stimulation of reduction by HPA. Figure 6 shows results from experiments in which HPA (200 μM) was premixed with C_1 before reaction with NADH in the stopped-flow instrument, and from those in which the same concentration of HPA was in the syringe containing NADH. These results showed that HPA must bind to C_1 before interacting with NADH to achieve maximal rate stimulation. Thus, the rate for binding of HPA to C_1 is slower than the rate of binding of NADH to C_1 or the C_1−HPA complex.

Kinetics of the Reduction of the C_1−HPA Complex by NADD. The reductions of the C_1−HPA complex by 4(*R*)-NADD and 4(*S*)-NADD were investigated and compared to the reduction by NADH (Figure 5A,B). A primary isotope effect on C_1−HPA reduction by 4(*S*)-NADD of 10 was observed, while the reduction by 4(*R*)-NADD was identical to that by NADH (data not shown). This indicates that C_1 is specific for the *pro*-(*S*)-hydride of NADH for reduction of the C_1-bound FMN. Kinetic traces of the 4(*S*)-NADD reaction at 458 and 690 nm were similar to those of NADH except that the reaction is many-fold slower (Figure 5). Data analysis indicated that only k_3(HPA) of Scheme 2 was changed, giving rise to the kinetic isotope effect of 10 (Table 1). Figure 5B shows that with 4(*S*)-NADD, less charge-transfer absorbance accumulates because the k_3/k_4 ratio in Scheme 2 is smaller than with NADH. Simulations with the same rate constants, except k_3 for NADD which equals 0.1 times the k_3 for NADH, are consistent with this interpretation (Figure 5).

Scheme 3

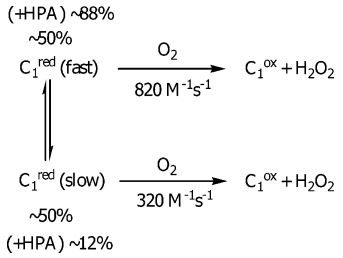

Reaction of Reduced C_1 with Oxygen. The reaction of reduced C_1 and oxygen was investigated by stopped-flow spectrophotometry in the presence and absence of HPA. The reduced enzyme was prepared as described in Materials and Methods and mixed with various concentrations of oxygen. The reactions were monitored at several wavelengths from 370 to 480 nm, and the results showed that the kinetics were similar at all wavelengths (data not shown). Traces of the reaction without HPA were biphasic, and both phases were comparable in amplitude. In the presence of HPA, the reaction is also biphasic, with the amplitude of the fast phase being ~88%, while the slow phase accounted for the rest (Figure 7 and Scheme 3). Further analysis showed that, in the presence or absence of HPA, the faster phase can be fitted with rates of 0.107 s^{-1} (130 μM oxygen), 0.267 s^{-1} (325 μM oxygen), 0.534 s^{-1} (650 μM oxygen), and 0.789 s^{-1} (960 μM oxygen), while the slower phase can be fitted with rates of 0.056 s^{-1} (130 μM oxygen), 0.105 s^{-1} (325 μM oxygen), 0.21 s^{-1} (650 μM oxygen), and 0.31 s^{-1} (960 μM oxygen). These rates are slower than the autocatalytic rate of oxidation of free reduced FMN under the same conditions (Figure 7). It should be noted that the reactions described above were carried out in the presence of superoxide dismutase (SOD) because the reactions without SOD were complicated by multiphasic kinetics. The rate of flavin

reoxidation was also slower in the presence SOD. Effects of SOD on the oxidation of C_1 suggested that the reaction with oxygen proceeded by a free radical mechanism that produces superoxide, similar to enzymes in the class of flavoprotein dehydrogenases (*36*).

DISCUSSION

This paper describes an investigation using transient kinetic methods of the reaction mechanism of the reductase component (C_1) of the two-protein HPAH system of *A. baumannii*. It clearly illustrates the important role of HPA in controlling the enzyme reaction with NADH. The flavin reduction with saturating NADH is stimulated by HPA by at least 30-fold (Table 1). In addition, the presence of HPA also increases the affinity of C_1 for NADH by more than 80-fold (Table 1). As a result of the combined changes to the reaction caused by HPA, the stimulus of reduction at 80−100 μM NADH is approximately 400-fold. The feature of a substrate or effector stimulating the reduction of enzyme-bound flavin by NADH is commonly found in the reactions of single-component aromatic flavoprotein hydroxylases such as *p*-hydroxybenzoate hydroxylase (*37*), anthranilate hydroxylase (*38*), 2-methyl-3-hydroxypyridine-5-carboxylic acid (MHPC) oxygenase (*39*−*41*), and 2-hydroxybiphenyl 3-monooxygenase (*42*). Thus, reduction by NADH is quite slow in the absence of the substrate effector. This is a means of preventing the wasteful oxidation of NAD(P)H and the consequent reaction of the E−FlH$^-$ complex with O_2 to form toxic H_2O_2 in the absence of an aromatic substrate (*7*, *37*). However, most of the two-protein flavoprotein hydroxylases were found not to exhibit this feature of control of reduction rate by effectors (*3*, *12*), with the notable exceptions of HPAH from *A. baumannii* (*4*) and *P. putida* (*2*) and NTA monooxygenase (*18*).

The stimulation by HPA of the reactions of C_1 is likely to occur through changes in protein conformation. When HPA is bound to C_1, the redox potential value of C_1 is lowered from −236 to −245 mV, making reduction thermodynamically less favorable. Therefore, the rate enhancement in flavin reduction cannot be due to thermodynamics. In the reduction reaction of single-component aromatic hydroxylases, thermodynamics are also not the cause of substrate-enhanced reduction by NAD(P)H; instead, it has been demonstrated that the binding of the substrate or effector optimizes the relative orientation of the enzyme-bound FAD for effective electron transfer from NAD(P)H (*37*). It can be envisaged that a similar concept could govern the function of C_1. The formation of prominent charge-transfer interactions between FMN and NADH in the presence of HPA (Figure 5) clearly demonstrates a close association that is also required for hydride transfer. Moreover, HPA changes C_1 from a mixture of enzyme species into an apparent homogeneous population readily reduced by NADH (Figures 4 and 5). Very similar phenomena were observed in the reduction of the flavoprotein component of HPAH from *P. putida* and the reductive half-reaction of 2-hydroxybiphenyl-3-monooxygenase, where the presence of HPA or 2-hydroxybiphenyl not only enhances the rate of NADH reduction but also changes the reduction kinetics from biphasic into monophasic traces (*5*, *42*). It has been proposed that the controlling effect of HPA on C_1 occurs through the additional C-terminal domain of the protein (*10*). A sequence corresponding to this domain is not found in reductases of other two-component enzyme systems, except for cB, which might be stimulated by the substrate, NTA (*18*).

The reaction of C_1^{red} with oxygen is ∼1 order of magnitude slower than the reaction of free FMNH$^-$ with oxygen (Figure 7) (*36*) and is unlikely to be related to any biological function of the protein. There are two possible explanations for the oxygen reactivity of C_1^{red} that are not easily distinguished experimentally. First, the protein environment of the flavin may inhibit its oxygen reactivity, as has been demonstrated for some nitroreductases (*43*) and medium-chain acyl-CoA dehydrogenase (MCAD) (*44*, *45*). Previous studies of MCAD have shown that the enzyme destabilizes formation of the superoxide anion intermediate by lowering solvent polarity at the active site environment (*44*, *45*). In such a case, binding of HPA might change the flavin environment from a mixture of two conformational species to a single species that is more reactive toward oxygen. An alternative explanation is that the protein environment inhibits the oxygen reactivity, and FMNH$^-$ must dissociate from the protein to react with oxygen. In this latter case, the low reactivity with oxygen would be due to the rate of dissociation of the flavin. In complex with HPA, C_1 might release the reduced flavin more readily, as suggested by the lower redox potential with HPA bound. This could be accomplished by increasing the off constant for flavin to promote a faster rate of reaction with oxygen. However, the kinetic evidence favors the first explanation, because of the approximately second-order behavior of the observed rate of reaction upon oxygen concentration.

The role of C_1 in the HPAH reaction is to provide reduced flavin for the oxygenase component (C_2) that hydroxylates HPA (*4*). Therefore, the ability of the substrate of the oxygenase (HPA) to control the reactivity of the reductase supplying reduced flavin to the system illustrates an interesting coordination of this two-protein system. At least three mechanisms have been proposed for transferring the reduced flavin from the reductase to the oxygenase component (*46*): (a) free diffusion of reduced flavin, (b) reduction of oxygenase-bound oxidized flavin by external reductants, including reduced flavin from the reductase, and (c) direct channeling from reductase to oxygenase in some form of complex. Recently, studies of the two-component monooxygenase involved in actinorhodin biosynthesis indicated that transfer of the reduced flavin was driven by thermodynamics (*25*). The oxygenase component has a higher affinity for reduced flavin than the reductase (*25*), thus favoring mechanism a. Our results with C_1 alone provide no definitive evidence for the mechanism of flavin transfer in the *A. baumannii* system. We will address this question in a future paper.

Only two of the known two-component oxygenase/reductase enzymes have been studied previously using rapid-reaction kinetics. Stopped-flow studies of the reductase of the NTA monooxygenase system have shown that the reduction of the cB-bound FMN by NADH was affected significantly by the His140Ala mutation (*47*). In wild-type reductase, the enzyme−NADH complex was formed with a K_d value of 20 mM, and the rate of hydride transfer was calculated to be 34.5 s^{-1} at 23 °C (*45*). This K_d value appears to be too high to be practical for physiological reactions. These properties are similar to the behavior of C_1 without HPA. The reductase of NTA monooxygenase (cB) has an

extra C-terminal domain similar to that of C_1. Surprisingly, the possible role of NTA in stimulating the rate of reduction in cB was not investigated in this study, although it was previously reported that NTA increased the rate of NADH oxidation in steady-state assays (*18*). Stopped-flow studies were also reported for the reaction of HPAH from *P. putida* (*5*). The reduction reaction of the FAD-bound component appeared to be similar to that of C_1 in many respects. In presence of HPA, the rate of FAD reduction by NADH was increased ~100-fold, and there was also evidence of formation of charge-transfer complexes between FAD and NADH during the reaction (*5*). Although HPAH from *A. baumannii* and *P. putida* may be quite different in the functional role of each protein component (*2*, *4*), both enzymes share the feature of having HPA as the modulator of the NADH reaction.

The studies presented here demonstrate that C_1 is a reductase utilizing the *pro*-(*S*)-hydride of NADH. This property is different from that of any of the known single-component aromatic hydroxylases, where all known enzymes in this class are specific for the *pro*-(*R*)-hydride of NAD(P)H (*48*). Known flavoenzymes specific for the *pro*-(*S*)-hydride of NAD(P)H are the disulfide oxidoreductases (*6*, *49*), suggesting that C_1 may be similar in some way to this class with respect to the binding geometry of pyridine nucleotide. The observed stereospecificity of reduction may be useful in structural studies of enzymes such as C_1.

In conclusion, our study has elucidated the reaction mechanism of C_1 and demonstrated the role of HPA as an effecter for stimulation of catalysis. Reported thermodynamic and kinetic constants can be used as a basis for understanding the reaction mechanism of the newly emerging class of reductases with an extra C-terminal domain. In a subsequent paper, we will demonstrate how these properties are utilized in the operation of the two-component system that achieves hydroxylation of HPA.

REFERENCES

1. Dagley, S. (1987) Lessons from biodegradation, *Annu. Rev. Microbiol. 41*, 1−23.
2. Arunachalam, U., Massey, V., and Vaidyanathan, C. S. (1992) *p*-Hydroxyphenylacetate-3-hydroxylase: A two-protein component enzyme, *J. Biol. Chem. 267*, 25848−25855.
3. Galan, B., Diaz, E., Prieto, M. A., and Garcia, J. L. (2000) Functional analysis of the small component of the 4-hydroxyphenylacetate 3-hydroxylase of *Escherichia coli* W: A prototype of a new flavin:NAD(P)H reductase subfamily, *J. Bacteriol. 182*, 627−636.
4. Chaiyen, P., Suadee, C., and Wilairat, P. (2001) A novel two-protein component flavoprotein hydroxylase: *p*-Hydroxyphenylacetate hydroxylase from *Acinetobacter baumannii*, *Eur. J. Biochem. 268*, 5550−5561.
5. Arunachalam, U., Massey, V., and Miller, S. M. (1994) Mechanism of *p*-hydroxyphenylacetate-3-hydroxylase: A two-protein enzyme, *J. Biol. Chem. 269*, 150−155.
6. Palfey, B. A., and Massey, V. (1998) Flavin-dependent enzymes, in *Comprehensive Biological Catalysis* (Michael, S., Ed.) Vol. 3, pp 83−153, Academic Press, San Diego.
7. Palfey, B. A., Ballou, D. P., and Massey, V. (1995) Oxygen activation by flavins and pterins, in *Active Oxygen in Biochemistry* (Valentine, J. S., Foote, C. S., Greenberg, A., and Liebman, J. F., Eds.) pp 37−83, Chapman & Hall, Glasgow, Scotland.
8. Xun, L., and Sandvik, E. R. (2000) Characterization of 4-hydroxyphenylacetate 3-hydroxylase (HpaB) of *Escherichia coli* as a reduced flavin adenine dinucleotide-utilizing monooxygenase, *Appl. Environ. Microbiol. 66*, 481−486.
9. Louie, T. M., Xie, X. S., and Xun, L. (2003) Coordinated production and utilization of $FADH_2$ by NAD(P)H-flavin oxidoreductase and 4-hydroxyphenylacetate 3-monooxygenase, *Biochemistry 42*, 7509−7517.
10. Thotsaporn, K., Sucharitakul, J., Wongratana, J., Suadee, C., and Chaiyen, P. (2004) Cloning and expression of *p*-hydroxyphenylacetate 3-hydroxylase from *Acinetobacter baumannii*: Evidence of the divergence of enzymes in the class of two-protein component aromatic hydroxylases, *Biochim. Biophys. Acta 1680*, 60−66.
11. Kim, I. C., and Oriel, P. J. (1995) Characterization of the *Bacillus stearothermophilus* BR219 phenol hydroxylase gene, *Appl. Environ. Microbiol. 61*, 1252−1256.
12. Kirchner, U., Westphal, A. H., Muller, R., and van Berkel, W. J. H. (2003) Phenol hydroxylase from *Bacillus thermoglucosidasius* A7: A two-protein component monooxygenase with dual role for FAD, *J. Biol. Chem. 278*, 47545−47553.
13. Gisi, M. R., and Xun, L. (2003) Characterization of chlorophenol 4-monooxygenase (TftD) and NADH:flavin adenine dinucleotide oxidoreductase (TftC) of *Burkholderia cepacia* AC1100, *J. Bacteriol. 185*, 2786−2792.
14. Louie, T. M., Webste, C. M., and Xun, L. (2002) Genetic and biochemical characterization of a 2,4,6-trichlorophenol degradation pathway in *Ralstonia eutropha* JMP134, *J. Bacteriol. 184*, 3492−3500.
15. Becker, D., Schrader, T., and Andreesen, J. R. (1997) Two-component flavin-dependent pyrrole-2-carboxylate monooxygenase from *Rhodococcus* sp., *Eur. J. Biochem. 249*, 739−747.
16. Otto, K., Hofstetter, K., Rothlisberger, M., Witholt, B., and Schmid, A. (2004) Biochemical characterization of StyAB from *Pseudomonas* sp. strain VLB120 as a two-component flavin-diffusible monooxygenase, *J. Bacteriol. 186*, 5292−5302.
17. Kadiyala, V., and Spain, J. C. (1998) A two-component monooxygenase catalyzes both the hydroxylation of *p*-nitrophenol and the oxidative release of nitrite from 4-nitrocatechol in *Bacillus sphaericus* JS905, *Appl. Environ. Microbiol. 64*, 2479−2484.
18. Uetz, T., Schneider, R., Snozzi, M., and Egli, A. (1992) Purification and characterization of two-component monooxygenase that hydroxylates nitrilotriacetate from *Chelatobacter* strain ATCC 29600, *J. Bacteriol. 174*, 1179−1188.
19. Xu, Y., Mortimer, M. W., Fisher, T. S., Kahn, M. L., Brockman, F. J., and Xun, L. (1997) Cloning, sequencing and analysis of a gene cluster from *Chelatobacter heiztzii* ATCC 29600 encoding nitrilotriacetate monooxygenase and NADH:flavin mononucleotide oxidoreductase, *J. Bacteriol. 79*, 1112−1116.
20. Witschel, M., Nigel, S., and Egli, T. (1997) Identification and characterization of the two-enzyme system catalyzing oxidation of EDTA in the EDTA-degrading bacterial strain DSM 9103, *J. Bacteriol. 179*, 6937−6943.
21. Eichhorn, E., van der Ploeg, J. R., and Leisinger, T. (1999) Characterization of a two-component alkanesulfonate monooxygenase from *Escherichia coli*, *J. Biol. Chem. 274*, 26639−26646.
22. Hastings, J. W. (1996) Chemistries and colors of bioluminescent reactions: A review, *Gene 173*, 5−11.
23. Lei, B., and Tu, S.-C. (1998) Mechanism of reduced flavin transfer from *Vibrio harveyi* NADPH-FMN oxidoreductase to luciferase, *Biochemistry 37*, 14623−14629.
24. Kendrew, S. G., Harding, S. E., Hopwood, D. A., and Marsh, E. N. (1995) Identification of a flavin:NADH oxidoreductase involved in the biosynthesis of actinorhodin. Purification and characterization of the recombinant enzyme, *J. Biol. Chem. 270*, 17339−17343.
25. Valton, J., Filisetti, L., Fontecave, M., and Niviere, V. (2004) A two-component flavin-dependent monooxygenase involved in actinorhodin biosynthesis in *Streptomyces coelicolor*, *J. Biol. Chem. 279*, 44362−44369.
26. Thibaut, D., Ratet, N., Bisch, D., Faucher, D., Debussche, L., and Blanche, F. (1995) Purification of the two-enzyme system catalyzing the oxidation of the *D*-proline residue of pristinamycin IIB during the last step of pristinamycin IIA biosynthesis, *J. Bacteriol. 177*, 5199−5205.
27. Parry, R. J., and Li, W. (1997) Purification and characterization of isobutylamine N-hydroxylase from the valanimycin producer *Streptomyces viridifaciens* MG456-hF10, *Arch. Biochem. Biophys. 339*, 47−54.
28. Duch, D. S., and Laskowski, M., Sr. (1971) A sensitive method for the determination of RNA in DNA and vice versa, *Anal. Biochem. 44*, 42−48.
29. Ottolima, G., Riva, S., Carrea, G., Danieli, B., and Buckman, A. F. (1989) Enzymatic synthesis of [4R-^{2}H] NAD(P)H and [4S-^{2}H]

NAD(P)H and determination of the stereospecificity of 7-α- and 12-α-hydroxysteroid dehydrogenase, *Biochim. Biophys. Acta 998*, 173−178.
30. Newton, C. J., Faynor, S. M., and Northrup, D. B. (1983) Purification of reduced nicotinamide dinucleotide by ion-exchange and high-performance liquid chromatography, *Anal. Biochem. 132*, 50−53.
31. Williams, C. H. J. R., Arscott, L. D., Matthews, R. G., Thorpe, C., and Wilkinson, K. D. (1979) Methodology employed for anaerobic spectrophotometric titrations and for computer-assisted data analysis, *Methods Enzymol. 62*, 185−198.
32. Massey, V. (1991) A Simple Method for the Determination of Redox Potentials, in *Flavins and Flavoproteins* (Curti, B., Rochi, S., and Zanetti, G., Eds.) pp 59−66, Water DeGruyter & Co., Berlin.
33. Loach, P. A. (1973) Oxidation−reduction potentials: Absorbance bands and molar absorbance of compounds used in biochemical studies, in *Handbook of Biochemistry Selected Data for Molecular Biology* (Sorber, H. A., Ed.) pp J-33−J-40, The Chemical Rubber Co. (CRC Press), Cleveland, OH.
34. Hiromi, K. (1979) Analysis of fast enzyme reactions: Transient kinetics, in *Kinetics of Fast Enzyme Reactions*, pp 193−194, Kodansha, Ltd. (Halsted Press), Tokyo.
35. Strickland, S., Palmer, G., and Massey, V. (1975) Determination of dissociation constants and specific rate constants of enzyme−substrate (or protein−ligand) interactions from rapid reaction kinetic data, *J. Biol. Chem. 250*, 4048−4052.
36. Massey, V., Palmer, G., and Ballou, D. P. (1971) On the reaction of reduced flavins and flavoproteins with molecular oxygen, in *Flavins and Flavoproteins* (Kamin, H., Ed.) pp 349−361, University Park Press, Baltimore.
37. Entsch, B., Cole, L. J., and Ballou, D. P. (2005) Protein dynamics and electrostatics In the function of *p*-hydroxybenzoate hydroxylase, *Arch. Biochem. Biophys. 433*, 297−311.
38. Powlowski, J., Ballou, D. P., and Massey, V. (1989) A rapid reaction study of anthranilate hydroxylase, *J. Biol. Chem. 264*, 16008−16016.
39. Chaiyen, P., Brissette, P., Ballou, D. P., and Massey, V. (1997) Thermodynamics reduction kinetics properties of 2-methyl-3-hydroxypyridine-5-carboxylic acid oxygenase, *Biochemistry 36*, 2612−2621.
40. Chaiyen, P., Brissette, P., Ballou, D. P., and Massey, V. (1997) Reaction of 2-methyl-3-hydroxypyridine-5-carboxylic acid (MHPC) oxygenase with *N*-methyl-5-hydroxynicotinic acid: Studies on the mode of binding, and protonation status of the substrate, *Biochemistry 36*, 13856−13864.
41. Chaiyen, P., Sucharitakul, J., Svasti, J., Entsch, B., Massey, V., and Ballou, D. P. (2004) Use of 8-substituted-FAD analogues to investigate the hydroxylation of the flavoprotein 2-methyl-3-hydroxypyridine-5-carboxylic acid oxygenase, *Biochemistry 43*, 3933−3943.
42. Suske, W. A., van Berkel, W. J. H., and Kohler, H. P. E. (1999) Catalytic mechanism of 2-hydroxybiphenyl 3-monooxygenase, a flavoprotein from *Pseudomonas azelaica* HBP1, *J. Biol. Chem. 274*, 33355−33365.
43. Koder, R. L., Haynes, C. A., Rogers, M. E., Rogers, D. W., and Miller, A.-F. (2002) Flavin thermodynamics explain the oxygen insensitivity of enteric nitroreductases, *Biochemistry 41*, 14197−14205.
44. Kim, J.-J., Wang, M., and Paschke, R. (1993) Crystal structures of medium chain acyl-CoA dehydrogenase from pig liver mitochondria with and without substrate, *Proc. Natl. Acad. Sci. U.S.A. 90*, 7523−7527.
45. Wang, R., and Thorpe, C. (1991) Reactivity of medium chain acyl-CoA dehydrogenase toward molecular oxygen, *Biochemistry 30*, 7895−7901.
46. Tu, S.-C. (2001) Reduced flavin: Donor and acceptor enzymes and mechanisms of channeling, *Antioxid. Redox Signaling 3*, 881−897.
47. Russell, T. R., and Tu, S.-C. (2004) *Aminobacter aminovorans* NADH:flavin oxidoreductase His140: A highly conserved residue critical for NADH binding and utilization, *Biochemistry 43*, 2887−2893.
48. Ballou, D. P. (1982) Flavoprotein Monooxygenases, in *Flavins and Flavoproteins* (Massey, V., and Williams, C. H., Eds.) pp 301−310, Elsevier North-Holland, New York.
49. Massey, V. (2000). The chemical and biological versatility of riboflavin, *Biochem. Soc. Trans. 28*, 283−296.

BI050615E